Graphene/Mo_2C heterostructure directly grown by chemical vapor deposition*

Rongxuan Deng(邓荣轩)[1,2], Haoran Zhang(张浩然)[1,2], Yanhui Zhang(张燕辉)[1], Zhiying Chen(陈志莹)[1], Yanping Sui(隋妍萍)[1], Xiaoming Ge(葛晓明)[1,2], Yijian Liang(梁逸俭)[1,2], Shike Hu(胡诗珂)[1,2], Guanghui Yu(于广辉)[1,†], and Da Jiang(姜达)[1,‡]

[1] *State Key Laboratory of Functional Materials for Informatics, Shanghai Institute of Microsystem and Information Technology, Chinese Academy of Sciences, Shanghai* 200050, *China*

[2] *University of Chinese Academy of Sciences, Beijing* 100049, *China*

(Received 10 January 2017; revised manuscript received 28 February 2017; published online 20 April 2017)

Graphene-based heterostructure is one of the most attractive topics in physics and material sciences due to its intriguing properties and applications. We report the one-step fabrication of a novel graphene/Mo_2C heterostructure by using chemical vapor deposition (CVD). The composition and structure of the heterostructure are characterized through energy-dispersive spectrometer, transmission electron microscope, and Raman spectrum. The growth rule analysis of the results shows the flow rate of methane is a main factor in preparing the graphene/Mo_2C heterostructure. A schematic diagram of the growth process is also established. Transport measurements are performed to study the superconductivity of the heterostructure which has potential applications in superconducting devices.

Keywords: graphene/Mo_2C heterostructure, CVD, methane flow rate, superconductivity

PACS: 79.60.Jv, 81.05.ue, 81.15.Gh, 74.70.–b **DOI:** 10.1088/1674-1056/26/6/067901

1. Introduction

Since the discovery of graphene in 2004,[1–4] many new two-dimensional (2D) materials have been found,[5–8] and 2D ultrathin Mo_2C is one of them.[9,10] Mo_2C belongs to the transition metal carbide, which combines the characteristics of ceramics and metals.[11,12] Mo_2C has not only high strength and hardness but also excellent catalytic activity and superconducting properties.[13] Scientists have fabricated large-area high-quality 2D ultrathin α-Mo_2C. The research of its physical properties, such as superconductivity and magnetotransport properties,[9,14] have achieved an important breakthrough.

Contemporarily, an important development trend in 2D material research field is the extension from a single material to an artificial heterostructure formed by two materials.[15–19] In the heterostructure, the superlattice periodic potential field caused by lattice mismatch exhibits a significant modulating action on the energy band structure of 2D materials. Moreover, it presents a novel quantum phenomenon which is not observed in single material.[20–23] Superconducting materials and graphene heterostructures, such as graphene/$Bi_2Sr_2CaCu_2O_{8+x}$ heterostructure, show an obvious nonlinear I–V characteristic, which indicates a possibility for developing the new superconducting devices.[24] Traditional 2D heterostructures are mainly prepared through a two-step process. This process includes either growing two materials in different conditions and then combining them to form a heterostructure, or growing one material directly onto another which is prepared as a substrate (epitaxial growth). Such a complicated preparation process tends to introduce contaminations at the interface and therefore has some limitations.

In this work, the graphene/ultrathin Mo_2C heterostructure is fabricated for the first time by one-step chemical vapor deposition (CVD) process, which can effectively avoid contaminations introduced in the traditional two-step growth process of heterostructure. The structure of heterostructure is verified. The key factor in fabricating the graphene/Mo_2C heterostructure and growth process is studied. The transport properties of the heterostructure are also measured.

2. Experiments

Cu (99.8% purity, 100-μm thick)/Mo (99.8% purity, 100-μm thick) foil as substrate were placed in a horizontal quartz tube furnace. Then, the samples were annealed under a flow of Ar/H_2 (5:1) at 1000 °C before growth to remove surface contamination. Subsequently, mixed methane, hydrogen, and argon gas were fed into the reaction chamber at different flow rates, with the temperature kept at 1086 °C. Upon the synthesis of heterostructure, the samples were then cooled down to

*Project supported by the National Natural Science Foundation of China (Grant Nos. 1402342, 11574338, and 11274333), the Hundred Talents Program of Chinese Academy of Sciences, the International Collaboration and Innovation Program on High Mobility Materials Engineering, Chinese Academy of Sciences (Grant No. KGZD-EW-303), and the "Strategic Priority Research Program (B)" of the Chinese Academy of Sciences (Grant No. XDB04040300).

†Corresponding author. E-mail: ghyu@mail.sim.ac.cn

‡Corresponding author. E-mail: jiangda@mail.sim.ac.cn

© 2017 Chinese Physical Society and IOP Publishing Ltd

room temperate naturally.

3. Results and discussion

Graphene/Mo_2C heterostructure can be fabricated using CVD under the following growth condition: 1-sccm CH_4, 200-sccm H_2, 1000-sccm Ar, 40 min, 100-μm Cu above 100-μm Mo. Figure 1(a) shows the typical optical microscope (OM) image of graphene/Mo_2C heterostructure which is confirmed in the text below. With the Raman spectrum of point A in Fig. 1(b), we confirm that the white hexagonal is a single-crystal graphene. The Raman spectrum of point B in Fig. 1(b) indicates that graphene is fabricated in the longitudinal direction of Mo_2C crystal.

We then confirm the structure of Mo_2C through several methods. Figure 1(c) shows the typical OM image of a hexagonal Mo_2C crystal without the graphene coating. It is proven to be composed of Mo and C by the typical energy-dispersive spectrometer (EDS) test as shown in Fig. 1(d). Figure 1(e) exhibits the high-resolution transmission electron microscopy (HRTEM) image of a part of the hexagonal sample which is randomly selected. From this figure, we calculate that the average spacing of lattice fringes is 0.26 nm. It is consistent with the (002) plane of α-Mo_2C crystal, confirming the existence of α-Mo_2C. As shown in Fig. 1(f), α-Mo_2C crystal has a really good single-crystal orientation.

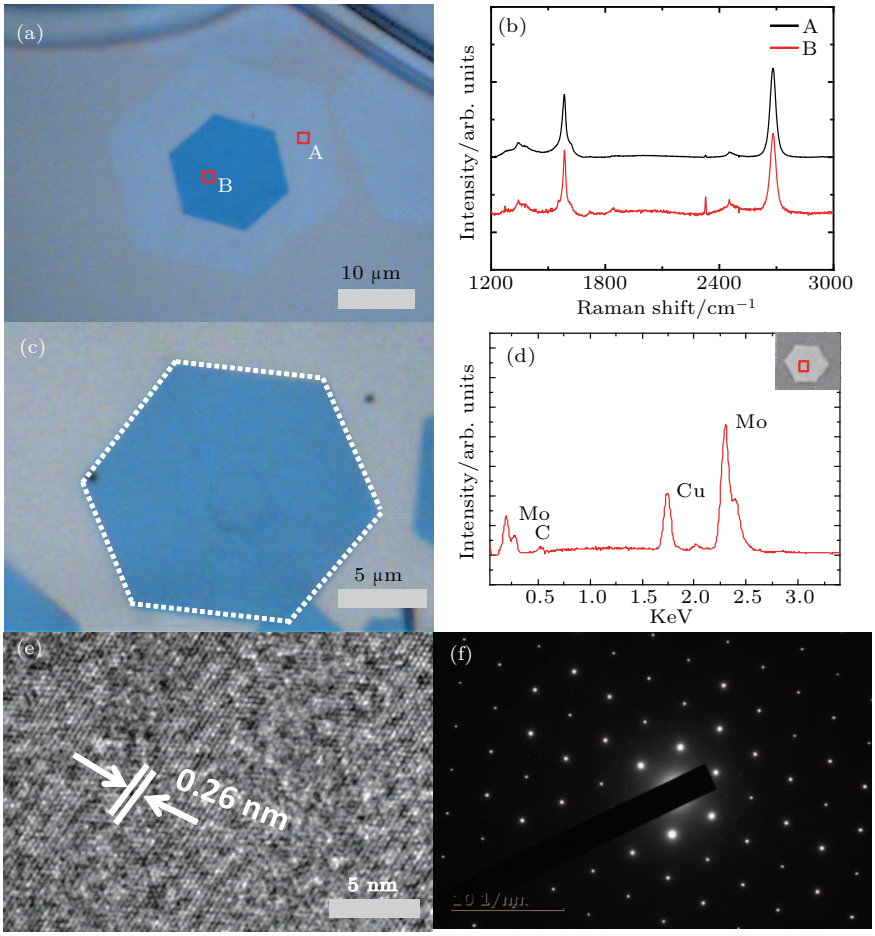


Fig. 1. (color online) (a) OM image of Mo_2C/graphene heterostructure. (b) Raman spectra of A and B, respectively. (c) Optical image and (d) typical EDS image spectrum of Mo_2C crystal fabricated by using CVD under the following condition: 1-sccm CH_4, 200-sccm H_2, 1000-sccm Ar, 40 min, and 100-μm Cu above 100-μm Mo. (e) HRTEM image and (f) SAED pattern of Mo_2C crystal. The inset in panel (d) shows the corresponding Mo_2C crystal (the same as those shown in panel (c)), and the red spot shows the position where the EDS spectrum is acquired.

Figure 2(a) shows the OM image of the sample with a methane flow rate of 0.35 sccm, where only Mo_2C crystal is grown. We cannot detect any Raman sign of graphene on the samples. In the case of low methane flow rate, the graphene cannot be fabricated on the molten copper. When the methane flow rate is increased to 1 sccm, the typical OM image is displayed as shown in Fig. 2(b). This condition is accompanied by the growth of hexagonal Mo_2C crystals and graphene. Part of hexagonal graphene completely covers the Mo_2C crystal. It demonstrates that Mo_2C crystal and graphene can be simultaneously grown and have the potential to form heterostructure under this condition. With the continuous increase of the methane flow rate to 2 sccm, the hexagonal graphene becomes a continuous graphene as shown in Fig. 2(c). The nucleation density and transverse dimension of Mo_2C crystal increase with the increase of methane flow rate. In summary, Mo_2C

crystal grows only at very low concentration of methane. The use of a high concentration of methane is the key to obtaining Mo_2C/graphene heterostructure.

Figure 2(d) shows a schematic diagram of the typical growth process for the heterostructure. In a horizontal quartz tube furnace, Cu foil (100-μm thick) is placed on the top of Mo foil (100-μm thick). The growth process is as follows: with the increase of temperature and upon the introduction of methane and hydrogen, methane splits into C–H atoms under the catalytic action of copper, and carbon turns into graphene on the surface of the molten copper. When the temperature reaches 1083.4 °C, copper melts with molybdenum atoms diffusing to the liquid copper to form copper/molybdenum alloy. Subsequently, carbon reacts with molybdenum to form molybdenum carbide. The hexagonal structure of Mo_2C crystal can be covered by the graphene to form a longitudinal heterostructure. The nucleation of molybdenum carbide and graphene on the copper surface randomly occurs, and there is no correlation between the nucleation positions. There are three kinds of position relationships between Mo_2C crystal and graphene within a certain time: hexagonal graphene completely covers Mo_2C crystals (see Fig. 2(b)), Mo_2C crystals are partially covered by graphene (Fig. 2(f)), and graphene and Mo_2C crystals are separated (Fig. 2(g)). With increasing time, the hexagonal graphene becomes continuous (Fig. 3(a)). In this case, each of the hexagonal structures of Mo_2C crystals can be covered by the graphene to form a longitudinal heterostructure.

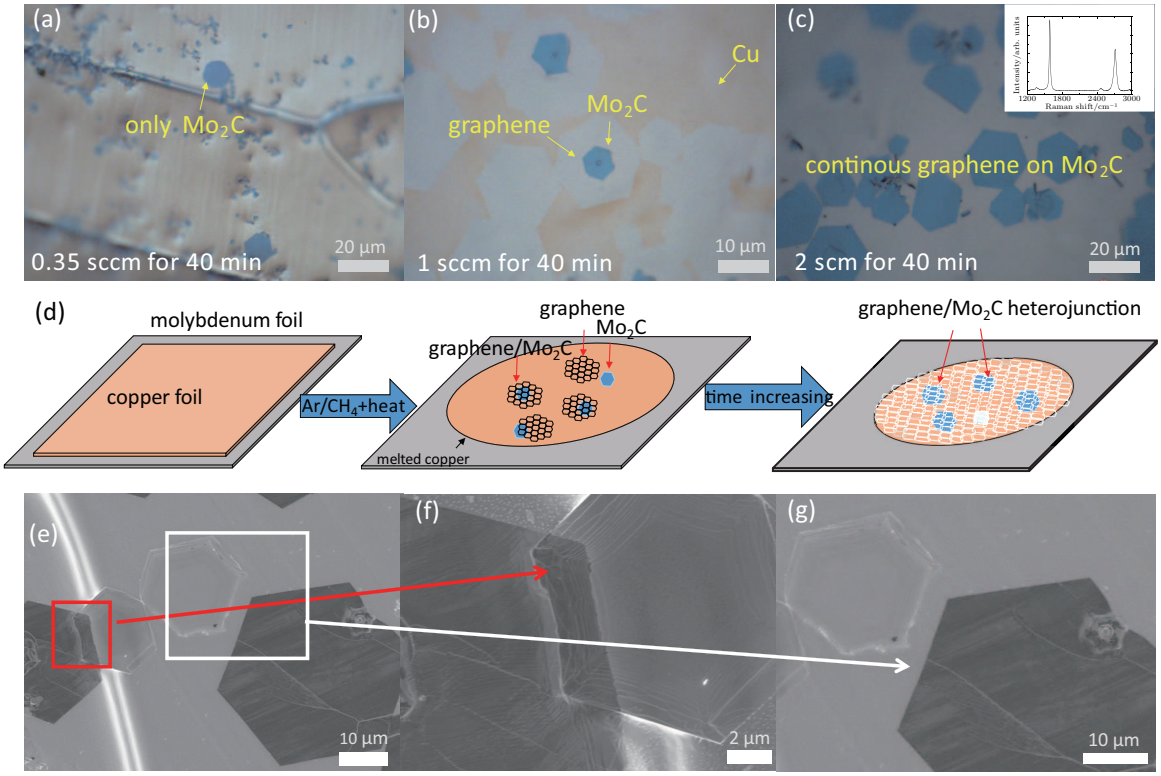


Fig. 2. (color online) OM images of samples after 40 min with methane concentrations of (a) 0.35 sccm, (b) 1 sccm, and (c) 2 sccm, respectively. The inset in panel (c) shows typical Raman spectra of a point on the top of the sample. (d) Schematic diagram of a typical heterostructure growth process. (e) SEM image of graphene and Mo_2C morphology under the following conditions: 1-sccm CH_4, 200-sccm H_2, 1000-sccm Ar, and 40 min; (f) SEM image of Graphene and morphology of Mo_2C stacked partially. (g) SEM image of graphene and morphology of Mo_2C separated.

The resulting heterostructures are transferred onto SiO_2/Si (300 nm/500 μm) substrates for characterization and application using a polymethylmethacrylate-supported transfer method.[25–27] Figure 3(a) exhibits the typical OM image of the transferred heterostructures. We verify the positional relationship between Mo_2C crystals and graphene with oxygen plasma etching after the transfer. Graphene can be etched by oxygen plasma under a certain condition (50 W, 2 min). A distinct crack is detected before oxygen plasma etching as shown in Fig. 3(a). A spot on the Mo_2C crystal corresponds to the Raman spectrum as shown in the inset; it demonstrates the existence of graphene. After the graphene film is etched, its crack disappears as shown in Fig. 3(b). The Raman spectrum of the spot in Fig. 3(b) shows that graphene is fully etched and removed, confirming that the graphene film is on the top of Mo_2C crystal. After transferring the graphene film onto Si_2O/Si substrate, we measure the thickness of heterostructure by atomic force microscope (AFM), and the thickness of heterostructure almost equals the thickness of Mo_2C crystal because the graphene on the Mo_2C crystal is too thin to be calculated according to the Raman spectrum shown in Fig. 3(a). The height profiles across the graphene/Mo_2C heterostructure shown in Fig. 3(d) demonstrate that the thickness of Mo_2C crystal is around 10 nm.

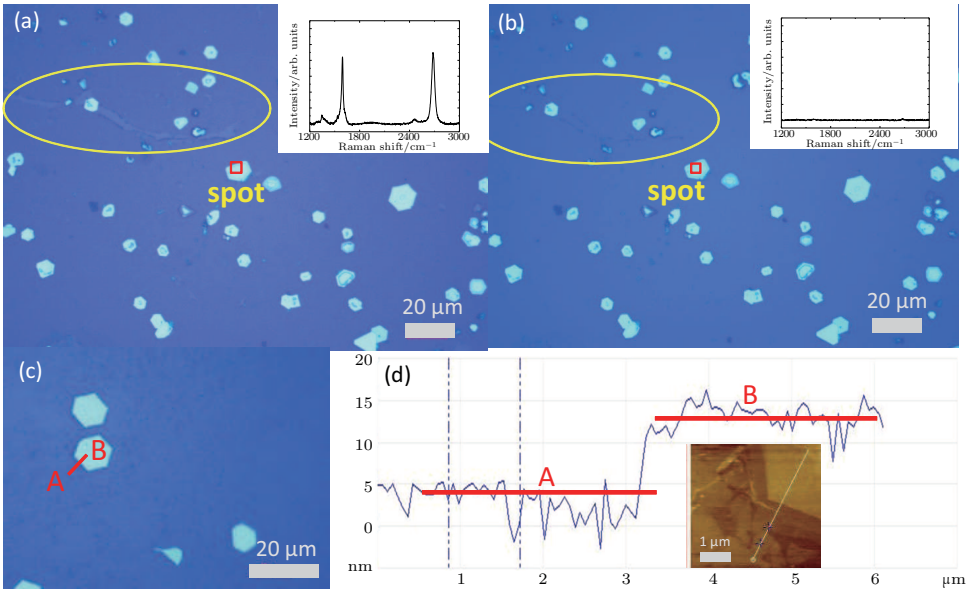


Fig. 3. (color online) OM image of one continuous graphene/Mo_2C heterostructure sample prepared under the conditions: 1-sccm CH_4, 200-sccm H_2, 1000-sccm Ar, 60 min, which is transferred onto a SiO_2/Si substrate (a). Graphene/Mo_2C heterostructure is etched by oxygen plasma afterwards (b). Insets in panels (a) and (b) show Raman spectra of the spot before and after etching, respectively. (d) AFM result for the typical graphene/Mo_2C heterostructure, showing the height profile along the red line in panel (c).

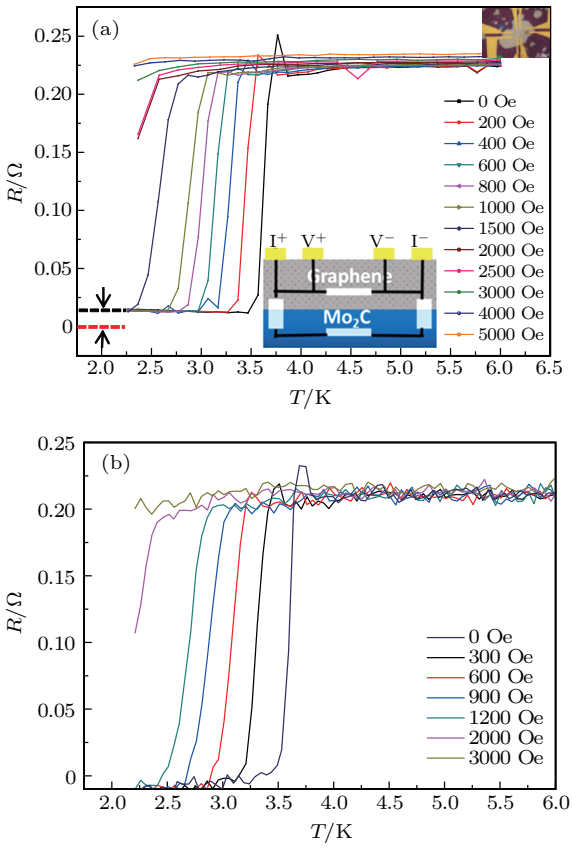


Fig. 4. (color online) Typical temperature dependence of resistance of graphene/Mo_2C heterostructure under various magnetic fields before (a) and after oxygen plasma etching (b). Inset in panel (a) shows an optical image of the device for transport measurement (upper left corner) and a brief circuit diagram of the transport measurement in the middle. The unit 1 Oe = 79.5775 A·m^{-1}.

Four-point probe measurement is performed on each of the graphene/Mo_2C heterostructure samples at the temperatures ranging from 2 K to 6 K by Physical Property Measurement System (PPMS, Quantum Design). Optical image of the device for transport measurement is shown in the inset of Fig. 4(a). Sharp resistive transition happening at around 3.7 K and magnetic field suppressing the superconductivity are shown in Fig. 4(a). It is worth noting that graphene and Mo_2C form a parallel circuit as shown in the inset of Fig. 4(a). The residual resistance can be detected through the gap between the red dashed and black dashed line in Fig. 4(a). It is the result of the current bypass effect of graphene[24] as shown by the circuit diagram. After getting rid of graphene by oxygen plasma etching (50 W, 2 min), Mo_2C remains superconductivity with zero resistance (Fig. 4(b)). This also verifies that graphene is on the top of Mo_2C flakes as an as-grown heterostructure.

4. Conclusions

In the present study, we successfully fabricate vertical graphene/Mo_2C heterostructure by using CVD directly. We summarize the growth rule of the heterostructure and find that Mo_2C crystals and graphene can be simultaneously grown with the high flow rate of methane and have the potential to form heterostructures. A schematic diagram of the growth process is also established. Finally, we study the superconductivity of the heterostructure after successfully transferring it onto Si_2O/Si substrate.

References

[1] Geim A K and Novoselov K S 2007 *Nat. Mater.* **6** 183
[2] Li X S, Cai W W, An J H, Kim S, Nah J, Yang D X, Piner R, Velamakanni A, Jung I, Tutuc E, Banerjee S K, Colombo L and Ruoff R S 2009 *Science* **324** 1312
[3] Mattevi C, Kim H and Chhowalla M 2011 *J. Mater. Chem.* **21** 3324
[4] Li X S, Cai W W, Colombo L and Ruoff R S 2009 *Nano Lett.* **9** 4268

[5] Bhimanapati G R, Lin Z, Meunier V, *et al.* 2015 *ACS Nano* **9** 11509
[6] Le Lay G, Salomon E, De Padova P, Layet J M and Angot T 2014 *Aust. J. Chem.* **67** 1370
[7] Nguyen H, Huang C F, Luo W J, Xia G R, Chen Z Q, Li Z Q, Raymond C, Doyle D and Zhao F 2016 *Mater. Lett.* **168** 1
[8] Zhang S Y, Zhang P G, Xie A J, Li S K, Huang F Z and Shen Y H 2016 *Electrochim. Acta* **212** 912
[9] Xu C, Wang L B, Liu Z B, Chen L, Guo J K, Kang N, Ma X L, Cheng H M and Ren W C 2015 *Nat. Mater.* **14** 1135
[10] Meshkian R, Naslund L A, Halim J, Lu J, Barsoum M W and Rosen J 2015 *Scripta Mater.* **108** 147
[11] Meyer S, Nikiforov A V, Petrushina I M, Kohler K, Christensen E, Jensen J O and Bjerrum N J 2015 *Int. J. Hydrogen Energy* **40** 2905
[12] Willens R H, Buehler E and Matthias B T 1967 *Phys. Rev.* **159** 327
[13] Cakir D, Sevik C, Gulseren O and Peeters F M 2016 *J. Mater. Chem. A* **4** 6029
[14] Wang L B, Xu C, Liu Z B, Chen L, Ma X L, Cheng H M, Ren W C and Kang N 2016 *ACS Nano* **10** 4504
[15] Bertolazzi S, Krasnozhon D and Kis A 2013 *ACS Nano* **7** 3246
[16] Tsai M L, Su S H, Chang J K, Tsai D S, Chen C H, Wu C I, Li L J, Chen L J and He J H 2014 *ACS Nano* **8** 8317
[17] Wang X M, Cheng Z Z, Xu K, Tsang H K and Xu J B 2013 *Nat. Photon.* **7** 888
[18] Su W J, Chang H C, Shih Y T, Wang Y P, Hsu H P, Huang Y S and Lee K Y 2016 *J. Alloys Compd.* **671** 276
[19] Huang J, Guo L W, Lu W, Zhang Y H, Shi Z, Jia Y P, Li Z L, Yang J W, Chen H X, Mei Z X and Chen X L 2016 *Chin. Phys. B* **25** 067205
[20] Ni G X, Wang L, Goldflam M D, Wagner M, Fei Z, McLeod A S, Liu M K, Keilmann F, Ożyilmaz B, Castro Neto A H, Hone J, Fogler M M and Basov D N 2016 *Nat. Photon.* **10** 244
[21] Ni G X, Zheng Y, Bae S, Tan C Y, Kahya O, Wu J, Hong B H, Yao K and Ozyilmaz B 2012 *ACS Nano* **6** 3935
[22] Ni G X, Wang H, Wu J S, Fei Z, Goldflam M D, Keilmann F, Ozyilmaz B, Castro Neto A H, Xie X M, Fogler M M and Basov D N 2015 *Nat. Mater.* **14** 1217
[23] Cao N T, Zhang L, Lü Lu, Xie H P, Huang H, Niu D Mei and Gao Y L 2014 *Acta Phys. Sin.* **63** 167903 (in Chinese)
[24] Jiang D, Hu T, You L X, Li Q, Li A, Wang H M, Mu G, Chen Z Y, Zhang H R, Yu G H, Zhu J, Sun Q J, Lin C T, Xiao H, Xie X M and Jiang M H 2014 *Nat. Commun.* **5** 5708
[25] Li X S, Zhu Y W, Cai W W, Borysiak M, Han B Y, Chen D, Piner R D, Colombo L and Ruoff R S 2009 *Nano Lett.* **9** 4359
[26] Liu N, Pan Z H, Fu L, Zhang C H, Dai B Y and Liu Z F 2011 *Nano Res.* **4** 996
[27] Fan Y, He K, Tan H J, Speller S and Warner J H 2014 *Chem. Mater.* **26** 4984